Journal of The Electrochemical Society, **149** (1) G70-G76 (2002)
0013-4651/2001/149(1)/G70/7/$7.00 © The Electrochemical Society, Inc.

Random and Ordered Macropore Formation in p-Type Silicon

A. Vyatkin,[a] V. Starkov,[a] V. Tzeitlin,[a] H. Presting,[b,z] J. Konle,[b] and U. König[b]

[a]*Institute of Microelectronics Technology, Russian Academy of Sciences, 142432 Moscow District, Chernogolovka, Russia*
[b]*DaimlerChrysler Research Center, D-89081 Ulm, Germany*

Random and ordered macropore formation in p-type silicon have been studied experimentally. We found that the density of macropores in a random macropore nucleation regime is linearly depending on the samples doping concentration. Macropore etching rate depends linearly on the current density up to the critical current density value; a saturation in the etching rate takes place when this value is exceeded. The so-called proximity effect was discovered for the ordered macropore formation regime. This phenomenon, and large pore diameters and pore wall thickness, and their variations have been observed in the experiments which can be accounted for in the frame of a simple model of the current localization at the pore bottom. An analysis of the experimental data based on the at present time existing theoretical models has been done. This analysis leads to the conclusion that none of these models can describe the existing experimental data including data of this work. It is clear that new experimental data are needed to come to a universal model of the electrochemical macropore formation.
© 2001 The Electrochemical Society. [DOI: 10.1149/1.1424898] All rights reserved.

Manuscript submitted February 26, 2001; revised manuscript received July 11, 2001. Available electronically December 6, 2001.

Macropore formation in silicon and other semiconductors using electrochemical etching processes has been, in the last years, a subject of great attention of both theory and practice. It is first due to new areas of macropore silicon applications arising from microelectromechanical systems processing (MEMS),[1-5] membrane techniques,[6-10] solar cells,[11] sensors,[12,13] photonic crystals,[14-18] and new technologies like a silicon-on-nothing (SON)[19] technology. A lot of experiments have been done on n-type silicon wafers and the theoretical model based on the role of the space charge region (SCR) (see, for example, the theoretical model made by Lehmann[20]). Only in the last five years has more attention been paid to macropore formation in p-type silicon.[21-30] However, only a few experimental groups have produced experimental data on the macropore formation in p-type silicon, while a number of theoretical models have been worked out to explain experimental dependencies observed. Among the more serious ones there are four models worth mentioning.

The first one belongs to Lehmann and Ronnebeck who tried to extend Lehmann's comprehensive model developed for macropore formation in n-type silicon to macropore formation in p-type silicon.[21] The model states that a silicon electrode anodized in hydrofluoric (HF) acid is under depletion in the regime of porous silicon formation and behaves, therefore, like a solid-state Schottky diode. As a result, macropore formation on p-type silicon can be understood as a consequence of the charge-transfer mechanisms in a Schottky diode if applied to a nonplanar interface. The forward current of a Schottky diode is dominated by either carrier diffusion, thermionic emission, or tunneling of holes. The model predicts that macropore formation on p-type silicon electrodes in HF solution is due to the increase of the diffusion current density at pore tips compared to flat electrode areas. The origin of this increase is the pore tip geometry, which produce a minimum of SCR width at the tip and consequently a maximum hole concentration gradient. Pore walls become passivated against dissolution if their distance decreases to two times the SCR width, because holes which initiate the dissolution process become depleted. Pore formation is suppressed according to the model if the charge transferred becomes dominated by the thermionic emission process, which is sensitive only to barrier height and not to barrier width. The model, as is seen, is valid only when pores are already formed and does not describe an initial stage of the macropore formation process.

The next model concentrated more on the early stages of porous silicon formation and was first proposed by Valance[25] and by Kang and Jorne,[26] and was developed by Ozanam *et al.*[24] The model based on linear stability analysis incorporates the transport phenomena of holes in the semiconductor and ions in the electrolyte. The model, as was shown by Ozanam *et al.*, predicts the characteristic structure sizes comparable with SCR width; however, the model cannot be used to describe the pore growth process in a proper way. Based on the same proposals, the model developed by Kang and Jorne resulted in a rather different conclusion: that the most likely dissolution mechanism during porous silicon formation involves the capture of two holes to form some intermediate silicon product Si(II) (this and next designations are taken from an article[31] which is discussed later in this paper), which further react with protons to produce Si(IV) and H_2 gas.

A model which pretends to account for all processes of the reactive Si-liquid interface including current oscillations on the current-voltage characteristics, is the formation of nano-, meso-, and macropores with their specific dependence on crystal orientation which has been recently proposed by Foll *et al.*[22] The model postulates that current flow across the solid silicon/HF-containing electrolyte interface is spatially and temporally inhomogeneous. Local current (it is called current burst) starts to flow whenever the local field strength is high enough. This current generates some oxide growth and it stops to flow at certain thickness of the oxide. Then, the oxide is dissolved purely chemically and whenever it is thin enough, the cycle starts again. These local events generally occur with random phases resulting in a constant macroscopic current, but under certain conditions, a percolation process may lead to a partial temporal and space synchronization and thus, to macroscopic current oscillations and to initiation of macropore formation. This model includes as well a process of H termination of free silicon surface. Moreover, the H termination process is the major synchronizing force for self-organized structure formation because it correlates the nucleation for current bursts. Since the H passivation process works fastest on {111} surfaces, these surfaces show a strongly reduced probability for generating current burst and thus for being etched. The model can predict some of the experimental results like frequency dependence of macropore parameter formation on external experimental parameters[31] but it is too general to be practically useful for many applications listed at the beginning of this introduction. For example, the model cannot predict pore diameter, pore wall thickness, pore formation rate, and other parameters which are of primary importance for practical applications.

The fourth model discussed here is a pure chemical model[32] which has been developed for n-type silicon, but can be applied to p-type silicon as well. In this kinetic model, unoxidized silicon surface atoms are represented by Si(0). At the first step of the anodic dissolution, Si(0) atoms capture a valence band hole according to the reaction

$$\mathrm{Si(0)} + h^{+}_{VB} \rightarrow \mathrm{Si(I)} \quad [1]$$

[z] E-mail: hartmut.presting@daimlerchrysler.com

Downloaded 08 Dec 2010 to 159.226.100.225. Redistribution subject to ECS license or copyright; see http://www.ecsdl.org/terms_use.jsp

It is assumed that the hole is captured in a Si-Si bond and the Si(I) intermediate state corresponds to a one-electron-deficient Si-Si back bond. This intermediate state is very mobile and can act as a catalyst for the dissolution reaction. The essential steps of the kinetic model can be summarized as follows

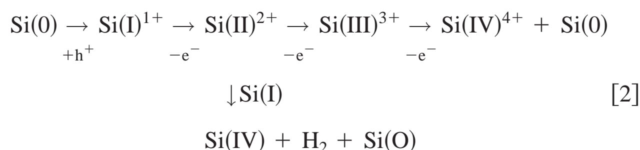

$$\mathrm{Si(0)} \underset{+h^+}{\rightarrow} \mathrm{Si(I)}^{1+} \underset{-e^-}{\rightarrow} \mathrm{Si(II)}^{2+} \underset{-e^-}{\rightarrow} \mathrm{Si(III)}^{3+} \underset{-e^-}{\rightarrow} \mathrm{Si(IV)}^{4+} + \mathrm{Si(0)}$$

$$\downarrow \mathrm{Si(I)} \quad [2]$$

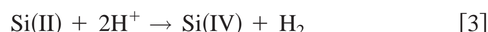

$$\mathrm{Si(IV)} + \mathrm{H_2} + \mathrm{Si(O)}$$

In the model, it is assumed that Si(I) stimulates the chemical reaction

$$\mathrm{Si(II)} + 2\mathrm{H}^+ \rightarrow \mathrm{Si(IV)} + \mathrm{H_2} \quad [3]$$

This would imply that anodic dissolution proceeds much faster in the surface region around an Si(I) intermediate state. Such an active region can be characterized by a radius which is determined by the diffusion length $L_{\mathrm{Si(I)}}$ of the mobile Si(I) intermediate. This diffusion length is defined as

$$L_{\mathrm{Si(I)}} = (D_{\mathrm{Si(I)}} \times \tau_{\mathrm{Si(I)}})^{1/2} \quad [4]$$

where $D_{\mathrm{Si(I)}}$ is the surface diffusion coefficient of the Si(I) intermediate and $\tau_{\mathrm{Si(I)}}$ is the lifetime. Inhomogeneous etching will occur if the diffusion length of the Si(I) intermediate is smaller than the average distance between these intermediates

$$L_{\mathrm{Si(I)}} < 1/s^{1/2} \quad [5]$$

where s is the surface concentration of Si(I) intermediates. Unfortunately, the model does not produce any estimations about the number of these intermediates.

Along with the models discussed briefly above, many other mechanisms of the macropore formation in p-type silicon have been proposed. Some of these mechanisms taking into the account the effect of the mechanical stresses which is either introduced during the electrochemical treatment of the semiconductors,[30] or has been introduced into the sample before electrochemical etching.[33]

At the present time, existing models and mechanisms of the macropore formation in silicon cannot explain all experimental data. Even the well-established Lehmann's model[20] developed for n-type silicon cannot explain the experimental data recently published.[34] Moreover, it seems very probable that the electrochemical process of macropore formation has a more universal nature and it is realized not only in semiconductors but in some metals as well, for example, in aluminum.[35-37] So, one can conclude that a deeper understanding of the electrochemical processes taking place during the macropore formation in materials requires more reliable experimental data.

In this paper, a wide range of experimental data related to macropore formation in p-type silicon and some discussion are presented.

Experimental

All experiments undertaken at the present work can be divided into two sets: random and ordered macropore nucleation and growth. Electrochemical etching of the p-type silicon has been performed in standard electrochemical cell with a sample area equal to 6 cm^2. A thin gold film about 15 nm thick vacuum deposited on the back side of the sample or InGa paste deposited by rubbing into the back side were used to provide uniform electrical contact. Current generator regime was used in all the experiments. The resistivity of the p-Si(100) samples studied varied in the range from 5 Ω cm to >1000 Ω cm. For the preparation of mixed solutions, 49% HF acid was used. Mainly two types of electrolytes were used in the experiments: $HF:H_2O:(CH_3)_2CHOH$ (isopropanol), 5:9:26, and HF:DMF (dimethylformamide), 1:10, solutions. To perform ordered macropore formation, an initial structure of ordered pitches has been produced by a preceding photolithographic process using standard potassium hydroxide (KOH) etching. To realize this technique, we have oxidized the silicon wafer with a SiO_2 layer the thickness of which varied in the range of 100-1000 nm depending on the pitch width required. Then photolithography with different photomasks has been carried out and finally, etching in KOH (30%) solution at 85°C has been used to produce an array of inverse pyramids etched into Si(100). Optical and scanning electron microscopy (SEM) have been used to analyze the pore diameter and the density of the pores.

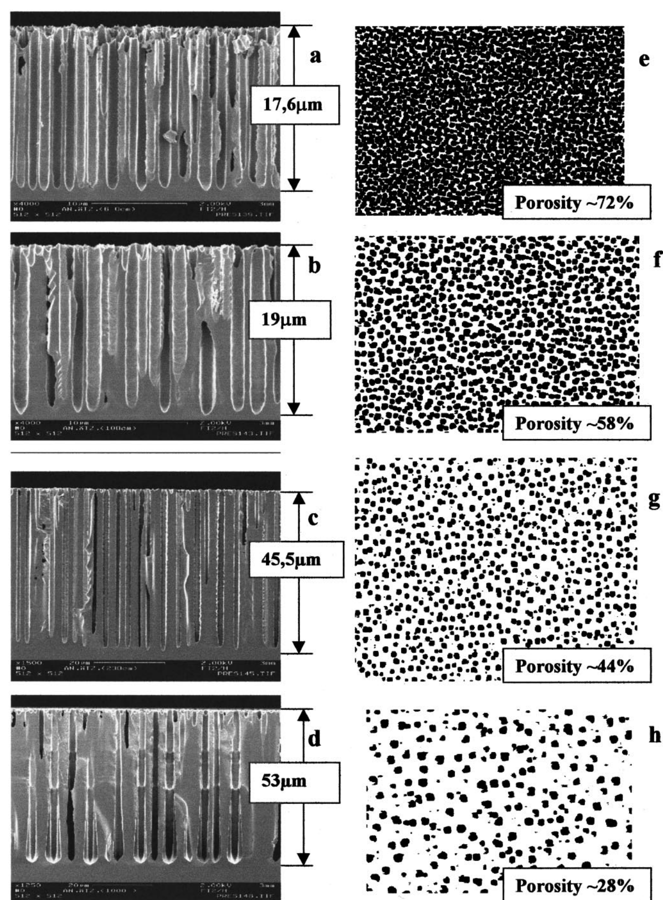

Figure 1. Random macropore formation in p-type silicon (SEM image): (a-d) Cross-sectional view taken from cleaves, (e-h) top plane view. Sample resistivity: (a, e) 6 Ω cm, (b, f) 10 Ω cm, (c, g) 23 Ω cm, and (d, h) 1000 Ω cm.

Results and Discussion

Random macropore formation.—Several experimental dependencies have been investigated in this part of the work. First, a dependence of the macropore diameter and etching rate on the resistivity of silicon samples has been observed. Figure 1 illustrates these dependencies. SEM images presented in Fig. 1 were taken as cross-sectional view of sample cleaves and top view. Si(100) samples with resistivities of 6, 10, and 23 Ω cm, and >1000 Ω cm were etched in HF:DMF (1:10) solution at room temperature with current density $J = 5.5\ \mathrm{mA/cm^2}$ for 60 min. The full set of the experimental data of this study is presented in Table I. The porosity was calculated using SEM top view images of the samples shown in Fig. 1e-h and used the Photo-Paint 8 computer program. J_p is the current density at the pore bottom and it was calculated according to the formula presented in the Table I, where J_{tot} is total current density, and A_p and A_{tot} are area of the pore cross sections and the total area of the plane surface of the sample, respectively.

Downloaded 08 Dec 2010 to 159.226.100.225. Redistribution subject to ECS license or copyright; see http://www.ecsdl.org/terms_use.jsp

Table I. Dependencies of pore diameter, etching rate, and surface porosity on sample resistivity.

Sample resistivity (Ω cm)	Pore diameter (μm)	Etching rate (μm/h)	Surface porosity (%)	$J_p = J_{tot} \times A_p/A_{tot}$ (mA/cm^2)
6	0.9	17.6	72	7.64
10	1.2	19	58	9.5
23	1.7	45.5	44	12.5
>1000	4.5	53	28	19.6

Dependencies of the macropore etching rate in p-Si(100) on the current density for two different electrolytes; HF:DMF based and $HF:H_2O:(CH_3)_2CHOH$ based are shown in Fig. 2. It is worth mentioning that data for HF:DMF etching were taken from a silicon sample with resistivity of 10 Ω cm, and data for the $HF:H_2O:(CH_3)_2CHOH$ etching were taken from a silicon sample with resistivity of 20 Ω cm. Dependence of the macropore density on doping concentration is presented on Fig. 3, where E is the density of the macropores in cm^{-2}, N is the doping concentration in atoms/cm^3, and m is the doping concentration at the surface in atoms/ cm^2. This plot contains the data taken from the present work and also the data taken from Ref. 21.

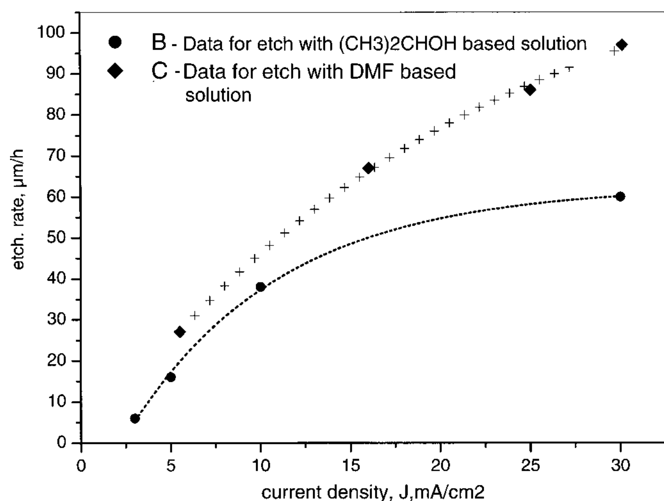

Figure 2. Macropore etching rate dependence on the current density.

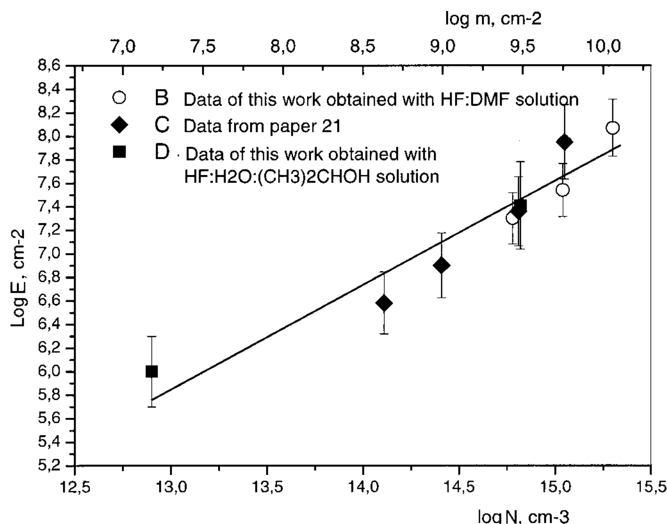

Figure 3. Macropore surface density, E, cm^{-2} dependence on bulk doping concentration, n, atoms/cm^3, bottom x axis, and on surface doping concentration m, atoms/cm^2, upper x axis.

It was shown as well that the pore diameter can be changed during the etch process by varying the current density. This effect can be clearly seen in Fig. 4 where a double-layer structure of p-type silicon (20 Ω cm) etched at two different current densities is shown: 10 mA/cm^2 (3.5 μm pore diam), and 30 mA/cm^2 (6 μm pore diam). Moreover, it was discovered that, if the first stage of such etching procedure is followed by etching with a current density of about 50 mA/cm^2, then the upper layer of the structure shown in Fig. 4 flakes off, producing a thin membrane with a network of holes with diam of 3.5 μm penetrating from top to bottom of this membrane. However, the pore diameter dependence on the current density is valid only when a pore structure has already been formed. If a varying current density is applied to the fresh samples without any preformed pore structure, then the pore diameter is constant for all current densities studied in this work (see Table II), whenever the sample resistivity is constant.

Ordered macropore formation.—Many applications of the macropore structures mentioned in the introduction of this paper require a macropore network which is ordered in space and is characterized by a given pore diameter. To meet these demands, a set of experiments with ordered macropore structures have been carried out. All experiments here were performed with an $HF:H_2O:(CH_3)_2CHOH$ (5:6:29) electrolyte. p-Type Si(100) wafers with resistivities in the range of 20 to >1000 Ω cm were used in the experiments. All data shown in this section of the work were obtained with silicon samples with resistivity >1000 Ω cm, but almost all of the results obtained for samples with resistivity of 20 Ω cm

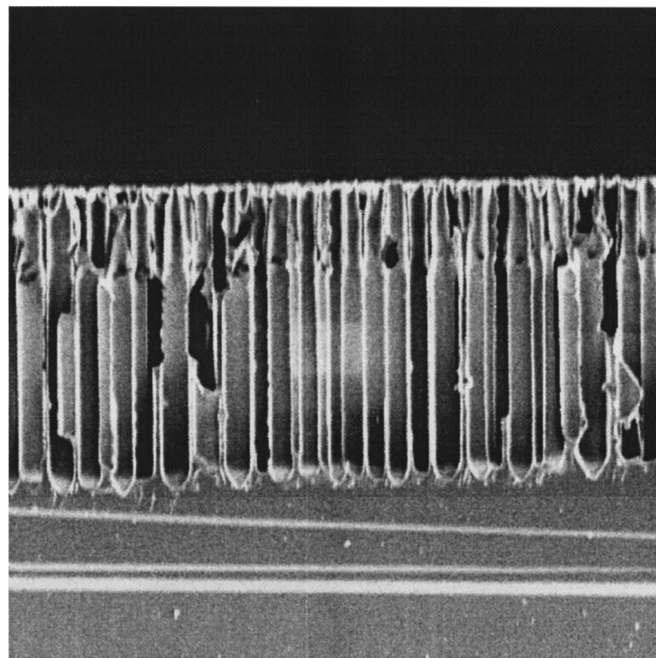

Figure 4. SEM image of double-layered structure of p-type silicon (20 Ω cm) etched at two different current densities. Upper layer, 10 mA/cm^2. Bottom layer, 30 mA/cm^2.

Downloaded 08 Dec 2010 to 159.226.100.225. Redistribution subject to ECS license or copyright; see http://www.ecsdl.org/terms_use.jsp

Table II. The pore wall thickness dependence on the current density.

Current density (mA/cm^2)	5.5	16	25	30
Pore diameter (μm)	1.1 ± 0.1	1.1 ± 0.1	1.1 ± 0.1	1.1 ± 0.1
Pore wall thickness (μm)	1.6	1.2	0.8	0.4

show the same behavior. SEM images in Fig. 5 demonstrate all steps of macropore formation procedure in prepatterned samples. Electrochemical etching has been done in this case at room temperature and a current density equal to 10 mA/cm^2. The photomask used for this purpose has open squares of 21×21 μm in size separated by 28 μm (edge to edge) as shown in Fig. 5a. The next step of the macropore formation is illustrated by the SEM image in Fig. 5b. It can be seen that deep and wide pores penetrate into the silicon sample according to the prepatterned inverse pyramid structure. However, in the areas between the inverted pyramids which were exposed to the electrolyte as well, random macropore nucleation and growth occurs. The diameter of these randomly nucleated pores is less than the pore diameter of the pores nucleated in the inverse pyramids, and is equal to the pore diameter characteristic for only random nucleated pores.

When the distance between the edges of two neighboring inverse pyramids becomes less than the pyramid width no random nucleation takes place in these areas. So, a strongly ordered structure consisting of single well distantly separated macropores can be produced. Figure 6 shows SEM images of different steps of such a structure formation (the distance between pyramid edges was equal to 4 μm). Electrochemical etching has been done in this case at a current density equal to 10 mA/cm^2 for 185 min at room temperature.

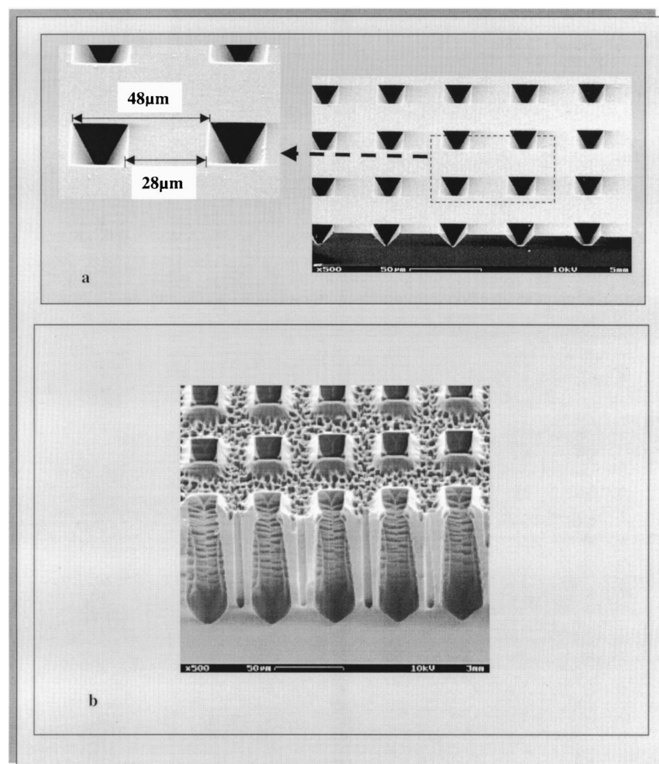

Figure 5. (a) SEM image taken from a Si(100) wafer after KOH etching. (b) The same sample after electrochemical etching in $HF:H_2O:(CH_3)_2CHOH$ (5:6:29) solution for 90 min, Current density equal to 10 mA/cm^2.

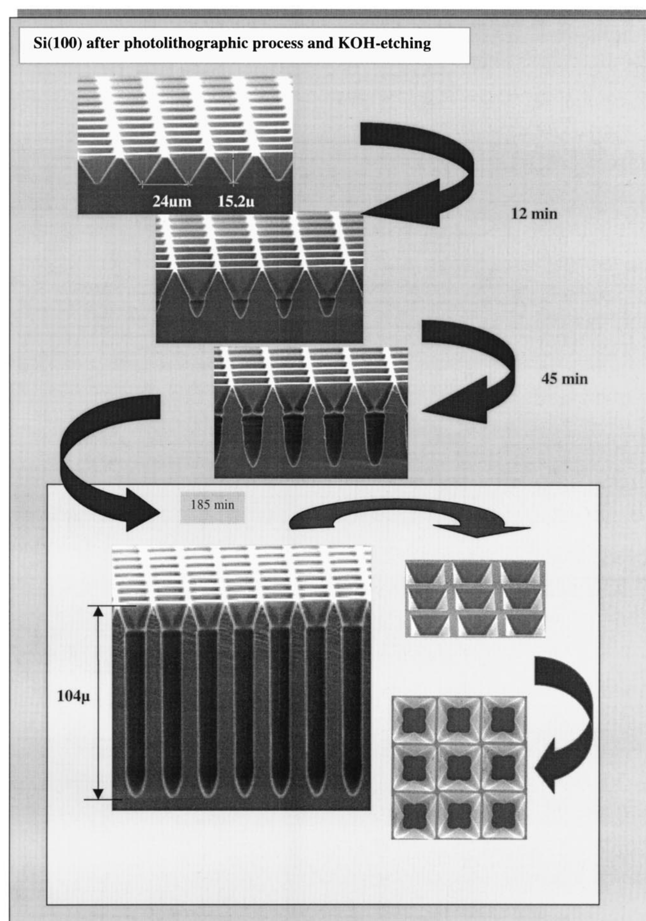

Figure 6. SEM images taken from Si(100) (>1000 Ω cm) samples illustrating deep macropore ordered formation. Etching parameters: electrolyte $HF:H_2O:(CH_3)_2CHOH$, current density $J = 10\ mA/cm^2$, $T = 21.5°C$, 185 min.

For the electrochemical etching conditions with no random nucleation, a well-pronounced pore diameter dependence on the current density can be observed (see Fig. 7). It is seen in Fig. 7 that the etching rate, is defined as etched pore depth per time, if it is only slightly dependent on the current density. Such macropore diameter dependence cannot be observed when the random nucleation between the pyramids takes place.

Using the pore diameter dependence on the current density, freestanding macroporous membrane with ordered macropore structures were produced as it is illustrated in Fig. 8.

Analysis of the experimental data presented above is done here, taking into account the theoretical models discussed in the introduction of the paper. It is accepted as a rule that the pore diameter is proportional to the wall thickness.[20,21] According to Lehmann's theory, the wall thickness is determined by the width of the SCR and the width of the SCR is proportional to the doping concentration. So, when the width of the SCR increases, the pore diameter increases as well. This statement can be used to account for the dependence which can be extracted from the first two columns of Table I which demonstrates the conclusion mentioned above. However, such behavior of the electrolyte/semiconductor system does not agree with the experimental data shown in Table II. The table shows that the wall thickness significantly decreases when the current density increases, while the doping concentration and the pore diameter are being constant which is in contradiction to Lehmann's

Downloaded 08 Dec 2010 to 159.226.100.225. Redistribution subject to ECS license or copyright; see http://www.ecsdl.org/terms_use.jsp

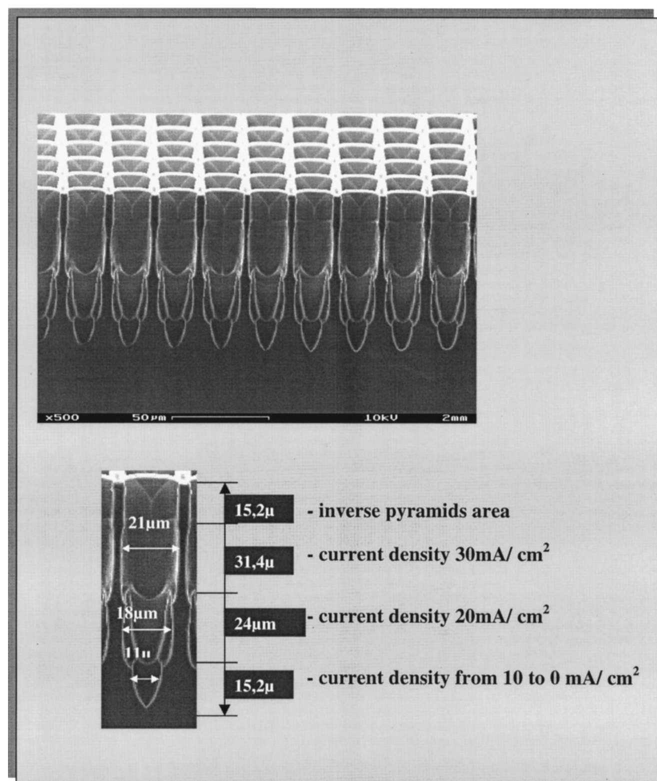

Figure 7. SEM image taken from Si(100) (>1000 Ω cm) sample after electrochemical etching at different current densities: first 30 min 30 mA/cm^2; next 30 min, 20 mA/cm^2; and last 30 min, 10 mA/cm^2. (For the last 10 min of these 30 min, current slowly decreases to 0 mA).

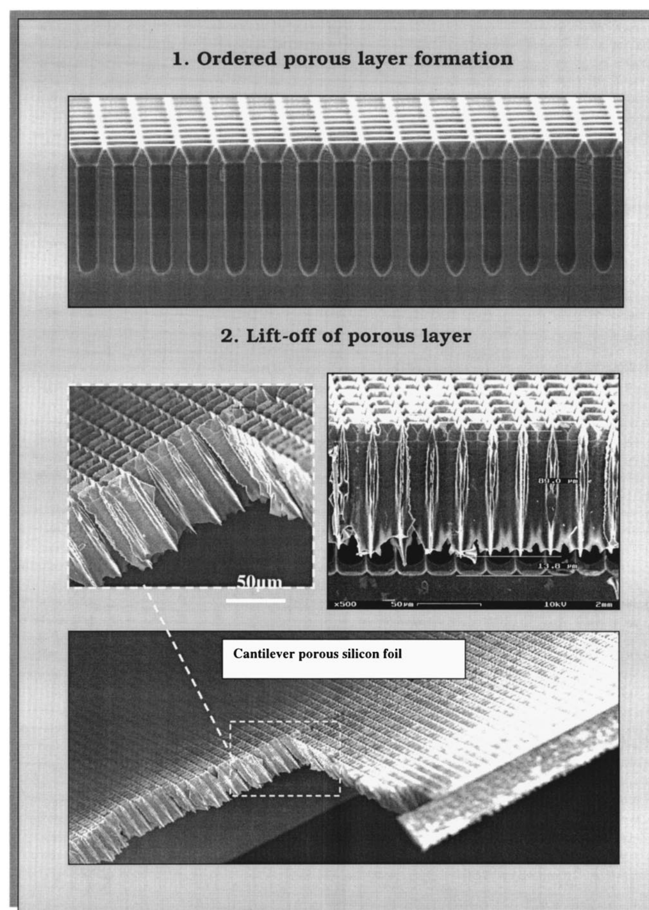

Figure 8. SEM images illustrating the freestanding membrane process flow.

theory. This can also clearly be seen in Fig. 4 and 7. It is shown that the pore diameter and hence the wall thickness are changed when the current density is varied. Meanwhile, following Lehmann's theory, the current density change has to result in a change of the etching rate while the pore diameter stays constant.

Etching rate dependencies on doping concentration and on current density are illustrated by the data in Table I (column 1 and 3) and by the data in Fig. 2. Figure 9 shows the etching rate dependence on the current density calculated on the basis of the data in Table I and according to the formula presented in Table I. All these data give clear evidence that up to certain value of the current density, a charge transfer across the electrolyte/semiconductor interface at the pore bottom is the dominating process in macropore formation in p-type silicon. This observation does not contradict with the model of "current bursts," proposed by Föll *et al.*[27]

However, as can be seen from Fig. 2 and 9, at a certain value of the current density, the etching rate saturates as a function of current density. This phenomena, and the fact that etching rate is dependent not only on current density but also on chemical composition of the electrolyte, clearly indicates the importance of the chemical reactions for the macropore formation process. The saturation of the etching rate (illustrated by Fig. 2 and 9) is strong evidence of the fact that, at certain value of the current density, the charge transfer process is not anymore a process which limits the macropore formation rate. What kind of chemical reaction not related to the charge transfer across the electrolyte/semiconductor interface is responsible for the macropore formation in this case? This is an open question and it cannot be answered on the basis of the experimental data of this work. However, the data of Ref. 38 show one example of such chemical reactions. It was shown that during a porous layer formation in the silicon-germanium epitaxial structure germanium redistribution occurs across an epitaxial layer. Because a solid-state diffusion can be excluded due to a room temperature pore formation process, one has to draw the conclusion that germanium atom transport in the electrolyte takes place, which is accompanied by a series of chemical reactions including germanium atom dissolution, diffusion, or mass transport in liquid electrolyte and deposition at the pore wall, far away from the dissolution site.

Some of the present experimental data can be as well accounted for taking into account the chemical model.[32] If we assume that

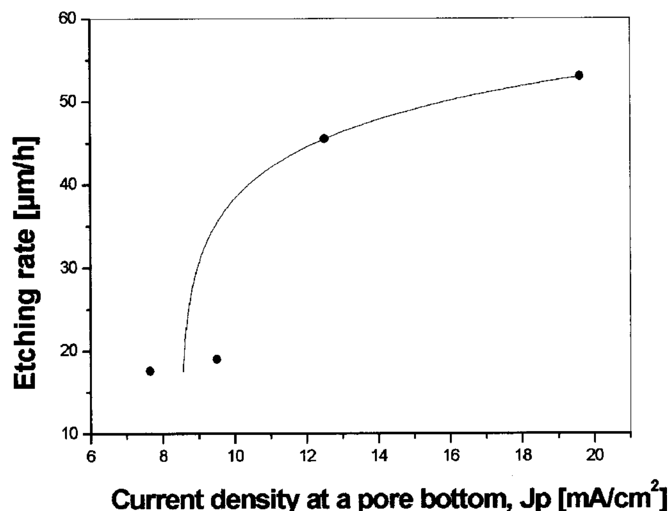

Figure 9. Macropore etching rate dependence on the current density at the pore bottom calculated and plotted from the data in Table I.

Downloaded 08 Dec 2010 to 159.226.100.225. Redistribution subject to ECS license or copyright; see http://www.ecsdl.org/terms_use.jsp

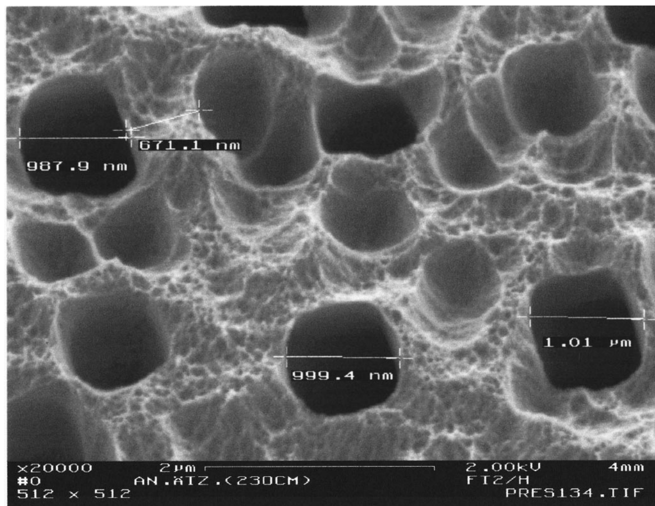

Figure 10. Top view SEM image taken from Si(100) (23 Ω cm) sample after electrochemical etching in HF:DMF solution at 23°C for 60 min and at current density $J = 5.5$ mA/cm^2.

chemical reaction with the catalytic participation of the Si(I) intermediates enhances at the surface sites where doping atoms are presented, *i.e.*, Si(I) intermediates are trapped at the doping atoms and hence diffusion length of such intermediates $L_{Si(I)}$ becomes much less that $1/s_I^{1/2}$ (this is a condition for inhomogeneous etching according to Ref. 32), then the surface density of the nucleated macropores have to be proportional to surface density of the doping atoms. Experimental data presented in Fig. 3 can be considered as a confirmation of this suggestion. It is seen that macropore density, log E, linearly scales with the doping concentration, log N. The upper axis in this plot is designated by log m which corresponds to the surface density of the doping atoms. This macropore nucleation process can be considered as well as a confirmation to the current burst model[27] if we assume that space synchronization of the current bursts occurs at the sites where doping atoms are present. It is seen as well that macropore density properly scales with the surface concentration of doping atoms. However, top-view SEM image taken from the sample with relatively high doping concentration (about 10^{15} cm^{-3}) presented in Fig. 10 which shows that only a part of the initially formed waviness on the sample surface causes the formation of deep macropores. This fact leads us to a suggestion that the pore nucleation and the pore growth processes are governed by different parameters of the electrochemical etching process.

So, these experimental data give some confirmation to the model described in Ref. 27 and 32, and give the arguments supporting some conclusions of the models, based on the linear stability analysis.[24-26] Indeed, Fig. 10 shows that not all of the surface perturbations initially nucleated result in macropore formation.

Ordered macropore formation results presented in Fig. 5-8 show that in a wide range of the silicon sample resistivities (20-1000 Ω cm) macropores with diameter and wall thickness significantly exceeding these for random nucleation can be produced. Moreover, macropore formation proceeds only in the areas where ordered etch pitches have been done by KOH anisotropic etching if the distance between two neighbor inverse pyramids is less than some critical value. For the silicon samples with resistivity varying in the above-mentioned range this critical value is within the range of 10–20 μm. This phenomenon can be called a "proximity effect," and large pore diameter and wall thickness observed do not seem to agree with the data for macropore random formation in silicon samples of the same resistivity. However, if a macropore formation process is considered as a process comprising two different stages, and if each of them is determined by different electrochemical etching parameters, then the above-mentioned experimental observations can be understood. Indeed, when an ordered macropore formation proceeds then the first stage of the process, *i.e.*, macropore nucleation, can be excluded from the consideration. So, the macropore formation process as a whole is only determined in this case by the macropore growth process. Analysis of the ordered macropore growth shows that the proximity effect and large pore diameter and wall thickness can be accounted for if we assume that all the current supplied to the sample is localized at the pore bottom until the current density at the pore bottom not reach some critical value. This critical value should have the same value as the current density value characteristic for the saturation regime in the etching rate *vs.* the current density dependence for random macropore formation regime (see Fig. 2 and 9). When the total current supplied to the sample is constant and the density of the KOH formed inverse pyramids is less than critical thickness in the proximity effect, then the current density at the pore bottom exceeds the critical value characteristic for the saturation regime. All extra current supplied to the sample then is consumed for macropore random nucleation in the areas between the inverse pyramids.

We have to conclude that random and ordered macropore formation in p-type silicon can be reasonably understood when the whole process is considered as a two-stage process comprising a macropore nucleation stage and a macropore growth stage. The macropore nucleation stage in the random macropore formation regime is governed to a high extent by chemical reactions in the electrolyte and is excluded in the ordered macropore formation regime. The macropore growth stage is about the same for both the random and ordered macropore formation regimes, and is determined up to some critical current density value by charge transfer at the pore bottom. When the current density is less than the critical current density, the variation in the current density results in the pore diameter change. When the current density is higher than critical current density value, then a random nucleation occurs between the ordered macropores, and an electropolishing takes place in the random nucleation regime.

Conclusions

Random and ordered macropore formation in p-type silicon has been studied experimentally. It was found that the density of macropores in a random macropore nucleation regime is linearly depending on the doping concentration of the sample. Macropore etching rate depends linearly on the current density up to the critical current density value and a saturation in the etching rate takes place when this value is exceeded. The so-called proximity effect was discovered for the ordered macropore formation regime. This phenomenon and large pore diameter and pore wall thickness and their variations observed in the experiments can be accounted for in the frame of a simple model of the current localization at the pore bottom. An analysis of the experimental data based on the at present time existing theoretical models leads to the conclusion that none of these models can describe completely the existing experimental data including the data of this work. And it is clear that new experimental data are needed to come to a universal model of the electrochemical macropore formation.

Acknowledgments

This work was supported by the R&G contract no. FT2/HS-4900037986 with DaimlerChrysler AG and research grant no. 00-02-17154 of the Russian Foundation for Basic Research.

DaimlerChrysler assisted in meeting the publication costs of this article.

References

1. V. Lehmann, in *Proceedings of IEEE MEMS Workshop '96*, p. 6 (1996).
2. H. Ohji, P. T. J. Gennissen, P. J. French, and K. Tsutsumi, *J. Micromech. Microeng.*, **10**, 440 (2000).
3. T. Laurell, L. Wallman, and J. Nilsson, *J. Micromech. Microeng.*, **9**, 369 (1999).
4. J. A. Walker, *J. Micromech. Microeng.*, **10**, R1 (2000).
5. V. Lehmann, W. Honlein, R. Reisinger, A. Spitzer, H. Wendt, and J. Willer, *Thin Solid Films*, **276**, 138 (1996).

Downloaded 08 Dec 2010 to 159.226.100.225. Redistribution subject to ECS license or copyright; see http://www.ecsdl.org/terms_use.jsp

6. K. J. Chao, S. C. Kao, C. M. Yang, M. S. Hseu, and T. G. Tsai, *Electrochem. Solid-State Lett.,* **3**, 489 (2000).
7. A. R. Angelucci, A. Poggi, L. Dori, A. Tagliani, G. C. Cardinari, F. Corticelli, and M. Marisaldi, *J. Porous Mater.,* **7**, 197 (2000).
8. M. K. Koukou, N. Papayannakos, N. C. Markatos, M. Bracht, N. M. Van Veen, and A. Roskam, *J. Membr. Sci.,* **155**, 241 (1999).
9. A. M. Rossi, G. Amato, L. Boarino, and C. Novero, *Mater. Sci. Eng.,* **B69-70**, 66 (2000).
10. J. von Behren, L. Trubeskov, and P. M. Fauchet, *Appl. Phys. Lett.,* **66**, 1662 (1995).
11. C. Levy-Clement and S. Bastide, *Z. Physicalische Chemie-Int. J. Res. Phys. Chem. Chem. Phys.,* **212**, 123 (1999).
12. R. Angelucci, A. Poggi, L. Dori, G. C. Cadinali, A. Parisini, A. Tagliani, M. Mariasaldi, and F. Cavani, *Sens. Actuators A,* **74**, 1 (1999).
13. C. M. A. Ashruf, P. J. French, P. M. Sarro, R. Kazinczi, X. H. Xia, and J. J. Kelly, *J. Micromech. Microeng.,* **10**, 505 (2000).
14. A. Chelnokov, K. Wang, S. Rowson, P. Garoche, and J.-M. Lourtioz, *Appl. Phys. Lett.,* **77**, 2943 (2000).
15. S. Rowson, A. Chelnokov, and J. M. Lourtioz, *Electron. Lett.,* **35**, 753 (1999).
16. S. Rowson, A. Chelnokov, and J. M. Lourtioz, *J. Lightwave Technol.,* **17**, 1989 (1999).
17. F. Miller, A. Birner, U. Gosele, V. Lehmann, S. Ottow, and H. Foll, *J. Porous Mater.,* **7**, 201 (2000).
18. U. Gruning, V. Lehmann, S. Ottow, and K. Busch, *Appl. Phys. Lett.,* **68**, 747 (1996).
19. I. Mizishima, T. Sato, S. Taniguchi, and Y. Tsunashima, *Appl. Phys. Lett.,* **77**, 3290 (2000).
20. V. Lehmann, *J. Electrochem. Soc.,* **140**, 2836 (1993).
21. V. Lehmann and S. Ronnebeck, *J. Electrochem. Soc.,* **146**, 2968 (1999).
22. J. Carstensen, M. Christophersen, and H. Foll, *Mater. Sci. Eng., B,* **69-70**, 23 (2000).
23. E. A. Ponomarev and C. Levy-Clement, *Electrochem. Solid-State Lett.,* **1**, 42 (1998).
24. J.-N. Chazalviel, R. B. Wehrspohn, and F. Ozanam, *Mater. Sci. Eng., B,* **69-70**, 1 (2000).
25. A. Valance, *Phys. Rev. B,* **55**, 9706 (1997).
26. Y. Kang and J. Jorne, *J. Electrochem. Soc.,* **144**, 3104 (1999).
27. M. Christophersen, J. Carstensen, A. Feuerhake, and H. Foll, *Mater. Sci. Eng.,* **B69-70**, 188 (2000).
28. G. Hasse, J. Carstensen, G. Popkirov, and H. Foll, *Mater. Sci. Eng.,* **B69-70**, 188 (2000).
29. C. Jager, B. Finkenberger, W. Jager, M. Christophersen, J. Carstensen, and H. Foll, *Mater. Sci. Eng.,* **B69-70**, 199 (2000).
30. V. Parkhutik, *Electrochim. Acta*, (2000), Accepted for publication.
31. H. Foll, J. Carstensen, M. Christophersen, and G. Hasse, in *Proceedings of the Porous Semiconductors 2000 Conference* (2000).
32. E. S. Kooij and D. Vanmaekelbergh, *J. Electrochem. Soc.,* **144**, 1296 (1997).
33. V. V. Starkov, E. A. Starostina, A. F. Vyatkin, and V. T. Volkov, *Phys. Status Solidi A,* **182**, 93 (2000).
34. P. Kleimann, J. Linnros, and S. Petersson, *Mater. Sci. Eng., B,* **69-70**, 43 (2000).
35. D. Routkevitch, T. Bigioni, M. Moskovits, and J. M. Xu, *J. Phys. Chem.,* **100**, 14037 (1996).
36. H. Masuda, H. Yamada, M. Satoh, H. Asoh, M. Nakao, and T. Tamamura, *Appl. Phys. Lett.,* **71**, 2770 (1997).
37. A. P. Li, F. Muller, A. Birner, K. Nielsch, and U. Gosele, *Adv. Mater.,* **11**, 483 (1999).
38. A. F. Vyatkin, J. Linnros, N. Lalic, and M. Rosler, *Phys. Low-Dimens. Semicond. Struct.,* **5/6**, 89 (1997).

Downloaded 08 Dec 2010 to 159.226.100.225. Redistribution subject to ECS license or copyright; see http://www.ecsdl.org/terms_use.jsp